




Micro-Ring Resonator Devices Prototyped on Optical Fiber Tapers by Multi-Photon Lithography

Vasileia Melissinaki, Odysseas Tsilipakos , Senior Member, IEEE, Maria Kafesaki , Maria Farsari, and Stavros Pissadakis 

Abstract—Multi-photon lithography -a powerful laser nanoscale additive-manufacturing method- is employed for structuring micro-ring traveling-wave resonators onto micrometric diameter, optical fiber tapers. These weakly guided, micro-ring resonating structures achieve light circulation with Q-factors of the order of $\sim 2.0 \times 10^3$, for typical diameters of tens of micrometers, in the spectral band of 1550 nm. The parametrization of the fabrication process, the characterization of these structures in TE and TM polarization, and the numerical simulation of their spectral performance is presented and analyzed. Moreover, these micro-ring resonators are exemplified into the demonstration of an ethanol vapor sensor, readily achieving detectivities of 0.5 ppm, based on reversible physisorption effects. Our demonstration aims at developing a new type of photonic platforms, based on a versatile, laser based prototyping approach onto micrometric size, optical fiber tapers, while exhibiting unique guiding and modal interaction characteristics, for departing the laboratory bench, while being implemented into diverse types of sensing and actuating devices.

Index Terms—Ethanol sensor, micro-ring resonators, multi-photon lithography, optical fiber sensors, optical fiber tapers.

I. INTRODUCTION

INTEGRATED micro-ring resonators (MRRs) [1], [2], are cornerstone devices in contemporary Photonics, offering access to tailored dispersion, high accumulation of circulated power and great sensitivity to refractive index and loss variations, necessary for developing numerous switching/routing [3]–[5], slow [6] and topological [7] light devices, as well as, sensors [8]. Planar geometry is inherently attractive in robustly accommodating bus waveguides and complex MRR structures on a single substrate, including cross-coupled or concatenated MRR cavities [6]. MRRs have also been investigated, in knotted

optical fibre tapers (OFTs) [9]; alternatively, whispering gallery mode (WGM) light resonating cavities have been infiltrated inside microstructured optical fibers [10], and exploited for nano-sensing applications [11]. While the above design approaches provide promising travelling wave light resonance functionalities, nonetheless, they rely on laborious fabrication protocols, which cannot be operated in a versatile prototyping fashion, for easily tuning the spectral response of the devices manufactured.

In general, the structuring of light resonating devices onto micrometric dimension OFTs (where optical connectorization is easy) for the realization of travelling wave photonic devices remains a great challenge, since the micrometric size and inherent fragility of OFTs do not allow the straightforward application of micromanipulation [12], nano-lithographic [13] or laser processing [14] methods. Thus, planar geometry still remains the preferable photonic host for developing and operating MRR devices.

Herein, we present a new kind of micro-photonic device platform, where MRRs are printed onto OFTs using multi-photon lithography (MPL). MPL is a laser-based 3D printing technique which allows the freeform fabrication of microstructures with sub-100 nm resolution [15]; including high complexity micro-optics [16], [17]. The use of MPL [18], [19] allows the imprinting of the MRRs directly onto the suspended OFTs, in a new approach of robust, micro-optical prototyping onto optical fibers [20]–[22], providing versatility in the fabrication of the resonating structures, whereas opening new prospects in the demonstration of novel micro-optical fiber devices. These micrometric diameter MRRs, are photo-imprinted onto silica glass OFT using an organic-inorganic hybrid negative resin, in a single step procedure, with the bus OFT exciting the MRR element in a fixed coupling condition; both the OFT and the attached MRR are suspended in air. The MRR-OFT devices presented here, are based on weakly guided waveguide elements of extended evanescent fields, necessary for sustaining a high overlap with the surrounding medium, or exhibiting enhanced sensitivity to minimal dimension surface perturbations introduced (i.e., monolayer physisorption effects). We further exemplify the capabilities of our MRR-OFT photonic design by developing an ultra-sensitive ethanol vapors sensor, readily measuring volume concentrations of 0.5ppm, while its transduction operation being based on reversible physisorption effects.

The primary objective of this work is the development of robust, high performance, and standard optical fiber connectorized MRRs on OFTs, with the goal of being packageable and

Manuscript received February 1, 2021; revised February 24, 2021; accepted February 24, 2021. Date of publication March 4, 2021; date of current version March 23, 2021. This work was supported in part by European Union's Horizon 2020 Research and Innovation Program LASERLAB-EUROPE under Grant 871124, ACTPHAST 4.0 under Grant 779472, and in part by HELLAS-CH under Grant MIS 5002735. (Corresponding author: Stavros Pissadakis).

Vasileia Melissinaki, Odysseas Tsilipakos, Maria Farsari, and Stavros Pissadakis are with the Institute of Electronic Structure and Laser (IESL), Foundation for Research and Technology-Hellas (FORTH), Heraklion, Greece (e-mail: melvas@iesl.forth.gr; otsilipakos@iesl.forth.gr; mfangari@iesl.forth.gr; pissas@iesl.forth.gr).

Maria Kafesaki is with the Institute of Electronic Structure and Laser (IESL), Foundation for Research and Technology-Hellas (FORTH), Heraklion, Greece, and also with the Dept. of Materials Science and Technology, Univ. of Crete, Heraklion, Greece (e-mail: kafesaki@iesl.forth.gr).

Color versions of one or more figures in this article are available at <https://doi.org/10.1109/JSTQE.2021.3062716>.

Digital Object Identifier 10.1109/JSTQE.2021.3062716

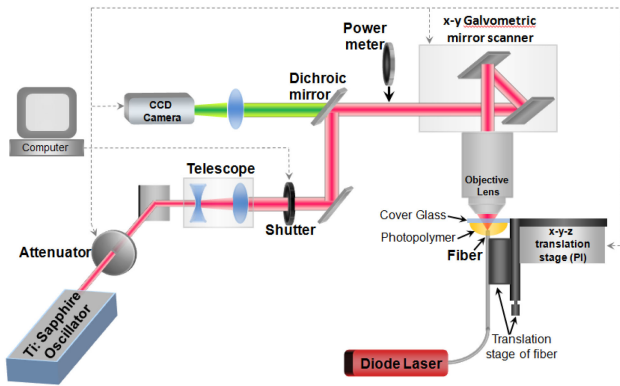


Fig. 1. Generic overview of the multiphoton lithograph 790 nm, femtosecond laser, 3D lithography experimental setup used for the structuring of the MRRs onto the OFTs.

potentially leaving the optical laboratory bench, for serving real field applications. The use of MPL for imprinting those MRRs onto the OFTs constitutes a strong asset of our approach, enabling the rapid prototyping of high surface and optical quality, travelling wave micro-phonic light resonating structures onto OFTs, into a fully three dimensional fabrication fashion. The above two optical engineering and laser prototyping advances constitute a two-fold paradigm for Industry 4.0 Photonics.

II. FABRICATION, CHARACTERIZATION AND SIMULATION DETAILS

A. Materials and MPL Setup

The material used for imprinting the MRRs, is an organic-inorganic hybrid composite, produced by adding zirconium propoxide (ZPO, 70% in propanol) to methacryl-oxypopyl trimeth-oxysilane (MAPTMS). MAPTMS and Dimethylaminoethyl methacrylate (DMAEMA) were used as the organic photo-polymerizable monomers, while ZPO and the alkoxy-silane groups of MAPTMS served as the inorganic network forming moieties. Michler's ketone, 44-bis(diethylamino) benzophenone (BIS), was used as a photo-initiator. All the chemicals were obtained from Sigma-Aldrich without any further purification. MAPTMS was first hydrolyzed using HCl solution (0.1 M) at a 1:0.1 ratio while ZPO was mixed with DMAEMA. After 15 minutes of stirring, the hydrolyzed MAPTMS was added to the zirconium solution at an 8:2 molar ratio and was left stirring for 10 minutes. The (MAPTMS+ZPO):DMAEMA molar ratio was 9:1. Finally, the photoinitiator was added to the mixture at a 1% w/w concentration in respect to the monomers. The final solution was magnetically stirred for 15 minutes before being filtered using a 0.22 μm pore size syringe filter, before exposure. The final photo-polymerised material after wet-development and nitrogen drying was estimated having a refractive index of $\sim 1.504 \pm 0.005$, at 1550 nm (1.52 at 589.3 nm [23]).

The MPL experimental set-up is shown in Fig. 1. A Ti:Sapphire femtosecond laser was employed as the light source (Tsunami, Model 3960-L3S, wavelength 790 nm, repetition rate of 80 MHz, pulse duration < 100 fs, 700 mW average power).

The laser beam was focused onto the sample through a high numerical aperture microscope objective lens (40x, N.A. = 0.95,

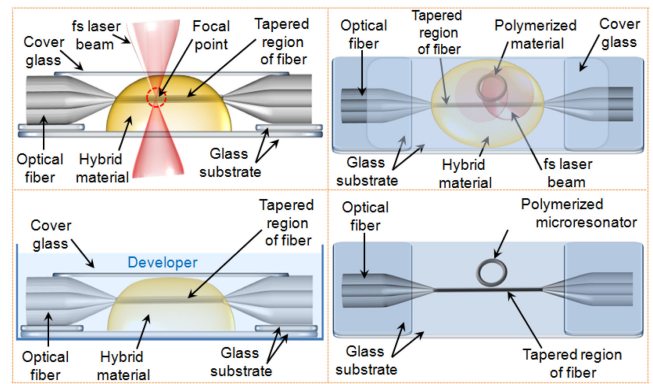


Fig. 2. Schematic representation of the MRR multiphoton lithograph fabrication process directly onto the OFT. The laser beam is focusing on the OFT-organic/inorganic resin material interface, where the photo-polymerization takes place only at the focal point of the laser beam (top-left). The non-linear laser photo-polymerization occurs within a single layer fashion (top-right). After the end of the photo-polymerization process the sample is developed in solvent in order the un-polymerized material to be washed off (bottom-left), revealing the final polymerized structure. (bottom-right).

Zeiss, Plan Apochromat), which was on a x-y galvanometric mirror digital scanner (Scanlabs Hurryscan II); before objective the laser beam was expanded 3x using a telescope lens. Z-axis scanning and larger-scale x-y movements were carried out using a high-precision (100 nm step) three-axis linear translation stage (Physik Instrumente-PI); together with an acousto-optic shutter. The beam alignment process with respect to the OFT was optically monitored by a CCD camera mounted behind a dichroic mirror. The lateral photopolymerisation resolution of the MPL system used here, was estimated to be ~ 160 nm.

The optical fiber tapers were fabricated using Corning SMF-28e standard telecom optical fiber and a Vytran GPX3000 glass processing station. Tapering was designed so to achieve adiabatic operation with typical taper waist length of 5mm and transition lengths of 21mm, each side, for a 2.2 μm diameter device. The OFT was then strained and attached using ultraviolet radiation activated epoxy, onto a structure of layered glass slides, of inverse pi-shape (see Fig. 2). For the MRR fabrication the resin material is drop casted on the OFT, then, had been left in ambient conditions to gelate. A small glass substrate of ~ 100 μm thickness was placed on the top of the epoxy droplet, in order to be used during the MPL process for the alignment.

The sample was left under vacuum conditions (22inHg) for at least 4 days to ensure solvent evaporation. For the fabrication of a 20 μm diameter micro-ring, the laser power was adjusted at 59 mW, while the galvanometric scanning speed was set at 2000 $\mu\text{m}/\text{sec}$, for 7 segmented scans.

The accuracy of positioning the MRR onto the OFT is limited by the imaging optics down to a figure of ~ 1.0 μm , rendering the actual optimization of the MRR excitation laborious. Depending on the desirable thickness of the ring, the beam was scanned inside the material in homocentric circles of 20 nm difference in their radius, with the largest radius being that of the desirable dimension of the MRR. After the end of the polymerizing process, the sample was immersed in a 70:30 solution of 1-propanol:isopropanol for at least 3 hours, to develop and remove un-polymerized material; then dried using nitrogen

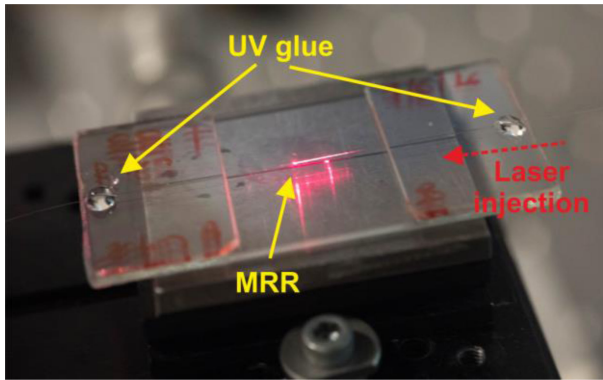


Fig. 3. Photograph of an MRR-OFT device, packaged onto a system of glass slides, while being injected with 650 nm laser light.

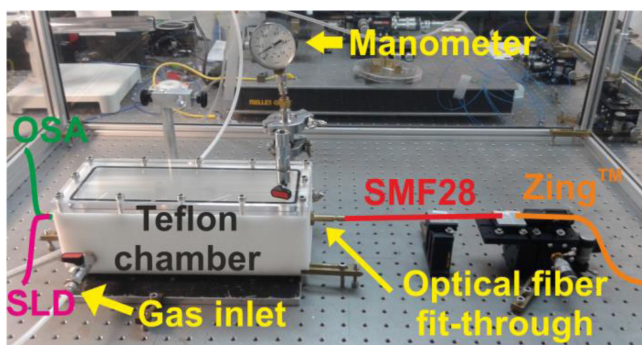


Fig. 4. Photograph of the Teflon chamber setup used for characterizing the MRR-OFT for different ethanol vapor pressures. Annotations explain optical fiber configurations and source/optical spectrum analyzer ports.

flow. The packaged device after wet development, is presented in Fig. 3.

B. MRR-OFT Ethanol Sensor Characterization Apparatus

A custom-made, gas tight, Teflon chamber, of 1400ml inner volume, was used for the pressure characterization of the MRR-OFTs ethanol sensor (see Fig. 4); a plexiglas window fitted on the top of the chamber allowed the optical inspection of the sample during the experiments. The chamber was fitted with tight seal optical fiber ports for performing transmission spectral measurements, while the MRR-OFT was kept under inert (Nitrogen) gas atmosphere. All measurements were carried-out with a super-luminescence light source (Q-Photonics) and traced using an optical spectrum analyzer (OSA) ANDO AQ6317B, and spectral resolution of 0.05 nm.

A 5 m long, Zing Polarizing Optical Fiber obtained from Fibercore was butt-coupled to the output SMF-28e port of the MRR-OFT, fitted onto a precision rotating V-groove for resolving TE and TM polarized spectra, with a polarization extinction ratio better than 30 dB. Suitable inlets and outlets were fitted in the Teflon chamber for the injection/pumping of gaseous species, together with a precision manometer allowing the measurement of changes in pressure due to ethanol evaporation. Measurements commenced from low to high concentrations, at a temperature of 22°C.

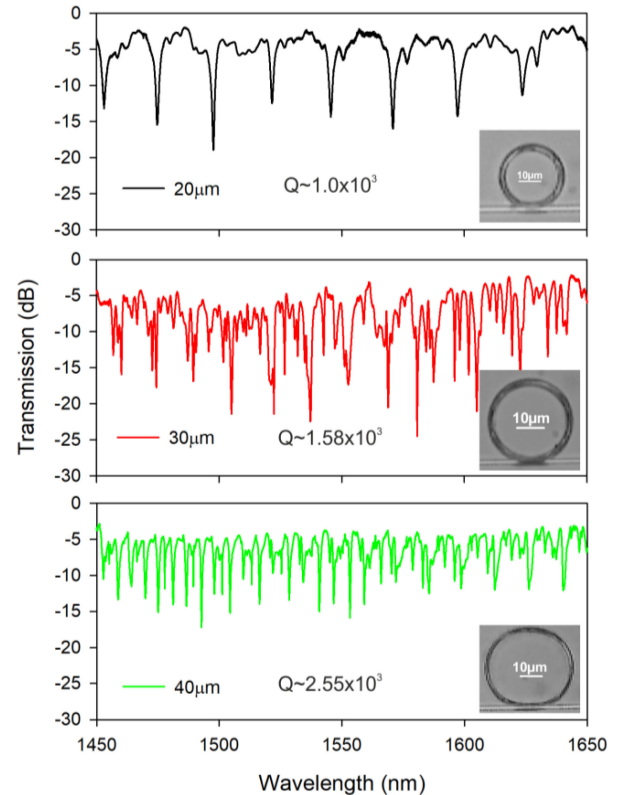


Fig. 5. Unpolarized transmission spectrum of MRRs of different ring diameter (see legends), photo-imprinted onto a 2.4 μm OFTs. Insets: optical microscope pictures.

C. Simulation Parameters

Full-wave simulations of the MRRs were performed with COMSOL Multiphysics 5.4, implementing the 3D vectorial finite element method (FEM). Frequency domain simulations were conducted to obtain reflection and transmission coefficients over the spectral range of interest, and eigenvalue simulations were used to identify the resonant modes of the MRRs [24].

III. RESULTS AND DISCUSSION

A. MRR-OFTs

MRR elements of varying geometrical characteristics were 3D-printed onto OFTs, while applying different exposure conditions. MRRs with diameters of 20, 30 and 40 μm were realized on $\sim 2.4 \mu\text{m}$ diameter tapers, with larger diameter MRRs exhibiting smaller free spectral ranges (FSR) and a spectral transmission richer in resonances (see Fig. 5); this is due to the longer cross-coupling length formed between the photopolymerized MRR and the OFT, promoting the efficient excitation of higher-vertical-order modes (see Fig. 8). Larger diameter MRRs also feature higher Q-factors, due to the reduction of bending losses of the ring waveguides. MRR structures with diameters larger than 40 μm appeared prone to self-collapsing, defining the limit with respect to the specific fabrication parameter.

After considering the spectral data of Fig. 5 and the overall mechanical stability of the photoinscribed structures, further

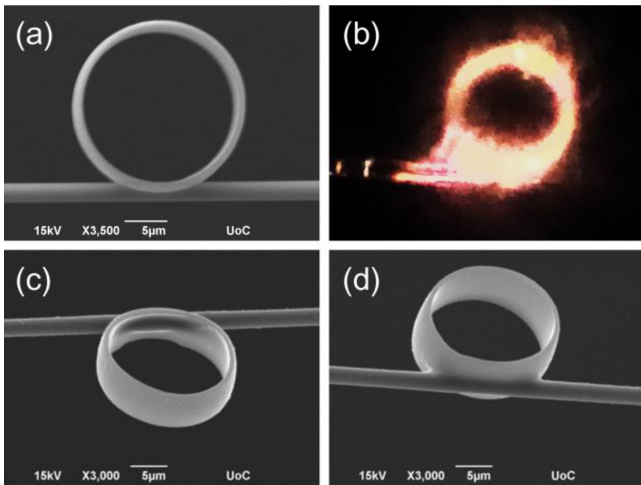


Fig. 6. (a), (c) & (d) Scanning electron microscope photographs of $20\ \mu\text{m}$ diameter MRRs fabricated using MPL onto OFTs. (b) Optical microscope picture of a $20\ \mu\text{m}$ diameter MRR while being excited using white light.

investigations were focused on $\sim 20\ \mu\text{m}$ diameter MRRs, simultaneously maintaining low curvature losses and adequate overlap between the bus OFT and the overlaid MRR. The specific MRR waveguides exhibit a transversally asymmetric shape ($\sim 8\ \mu\text{m}$ height, $\sim 0.8\ \mu\text{m}$ thickness), introducing a strong polarization sensitivity; the dimensional characteristics of the inscribed MRRs, are largely defined by the objective NA and the photoresist used (see Fig. 6). For mechanical stability reasons, the MRR is highly overlapped with the OFT, leading to an over-coupled excitation scheme [25] in cost of the resonance Q-factor and extinction ratio of the spectral resonances. Controlling the coupling conditions of the MRR by adjusting its position onto the OFT was attempted, however the actual control over this process is still rather limited, due to the resolution of the optical system used.

The asymmetric geometrical characteristics, as well as the particular coupling condition applied in those MRRs are directly manifested into the resonant spectra measured for TE (electric field perpendicular to the structure plane) and TM (magnetic field perpendicular to the structure plane) polarization states (see Fig. 7).

The highest Q-factors measured for a $\sim 20\ \mu\text{m}$ diameter ring attached onto a $2.2\ \mu\text{m}$ OFT, are of the order of 2.4×10^3 for the 53rd azimuthal order TM mode located at 1583 nm (Q-factors smaller than 1.0×10^3 generally hold for an equal order TE mode), and typical free spectral ranges (FSRs) between major notches are $\sim 25.4\ \text{nm}$ (see Fig. 7). The optical absorption and scattering of the photoresist and eccentricity/thickness variations of the MRRs do not allow for obtaining higher Q-factors.

Employing rigorous 3D Finite Element Method simulations [24], we can reproduce the measured spectra (Fig. 8). The structure of the transmission curve includes sharp main dips, associated with the excitation of the first-vertical-order ($q = 1$) resonant modes with different azimuthal order. There are also secondary dips associated with higher vertical orders ($q = 2$ and $q = 3$); note that we have opted for a narrow MRR, in order to

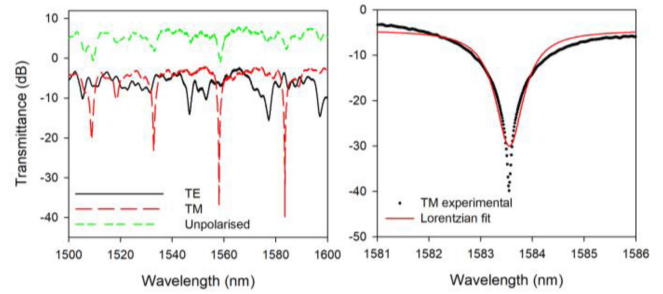


Fig. 7. (left) Polarisation resolved and unpolarised transmission spectra of a $20\ \mu\text{m}$ diameter MRR-OFT. The unpolarised spectra have been shifted up by 10 dB for allowing comparison. (right) Close view of a $20\ \mu\text{m}$ diameter MRR-OFT resonance for TM polarization; solid line represents a Lorentzian fitting with a bandwidth factor of 0.328 nm.

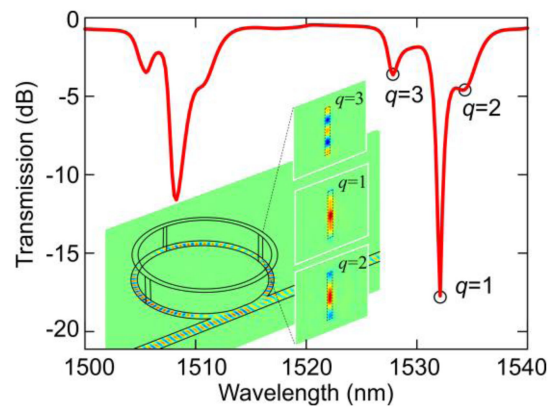


Fig. 8. Transmission spectrum for TM polarization, as obtained from 3D vectorial Finite Element Method simulations for a rectangular cross-section ring resonator with dimensions $800\ \text{nm} \times 8\ \mu\text{m}$ attached onto a $2.2\ \mu\text{m}$ diameter OFT. Transmission dips associated with resonant modes of different vertical order ($q = 1, 2, 3$) are identified. The inset depicts field distributions of the 3D simulations in xy and xz cut-planes. The different vertical orders of the field distributions at the frequencies of the marked dips are clearly shown.

suppress higher radial orders. The above are illustrated in Fig. 8, where we focus in the on TM polarization and wavelength range 1500–1540 nm, including two first-vertical-order dips with a free spectral range of 24 nm in perfect agreement with the experiment.

The field distributions verifying the excitation of the different resonant modes are included as insets, clearly showing the different vertical order resonances that are excited in the MRR structure, leading to the respective dips marked in Fig. 8. Note that in principle higher order resonances along the radial direction could be also excited in the MRRs. However, since the thickness of the MRR is only 800 nm, such resonances are characterized by high radiation leakage and thus if excited do not produce sharp spectral signature (see Fig. 7 and 8).

B. MRR-OFT Ethanol Vapor Sensor

Following the above realizations, a $20\ \mu\text{m}$ diameter MRR onto a $2.2\ \mu\text{m}$ OFT, was manufactured for testing its response to ethanol vapors at low concentrations. The choice of ethanol as a testbed gas for checking the physisorption response of the

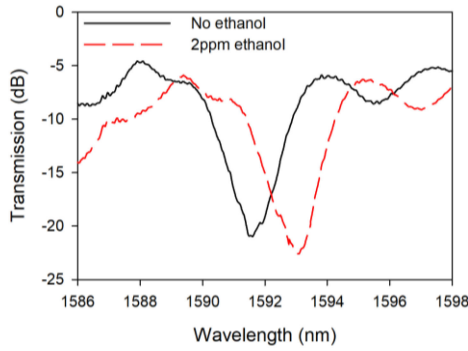


Fig. 9. Transmission spectra of a TM polarisation MRR mode at 1591.54 nm, been measured in 1.0bar nitrogen atmosphere (black line) and after 7 min exposure to 2ppm ethanol vapor stimulation.

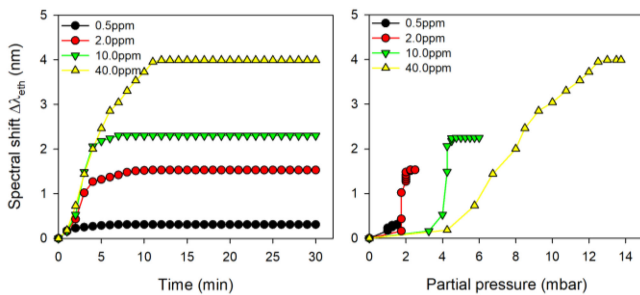


Fig. 10. (left) Ethanol vapor induced spectral shift $\Delta\lambda_{eth}$ of the MRR-OFT system versus exposure time to ethanol vapors. (right) Ethanol vapor induced spectral shift $\Delta\lambda_{eth}$ of the MRR-OFT system versus partial pressure of ethanol vapors inside the characterization chamber. Experimental error for the $\Delta\lambda_{eth}$ spectral shift: 0.05 nm. Experimental error for the partial pressure: 0.5mbar.

MRR-OFT device was based on several previous studies [26] with the same photopolymerised resin (in different resonating devices [21]), planar micro-ring resonators [27] and other transducers (ie ZnO [28]). In addition, ethanol concentration in ppm levels detected in human breath is related to the onset of a number of metabolic [29] and neoplasia [30] diseases, rendering the development of miniature size, yet highly-sensitive probe devices clearly impactful.

For performing the ethanol sensing experiments a TM polarization mode resting at ~ 1591.54 nm was selected for being probed under ethanol vapor stimulation; its strength as fabricated was ~ 15 dB, while its Q-factor was measured to be $\sim 0.58 \times 10^3$ (see Fig. 9). Upon exposure of this ring resonating optical fiber taper system to i.e., 2.0ppm ethanol concentration, the resonance mode examined, started red-shifting, then reaching a maximum ethanol induced spectral shift $\Delta\lambda_{eth}$ of 1.5 nm; lower ethanol concentrations down to 0.5ppm ($\Delta\lambda_{eth}^{0.5ppm} = 0.3$ nm) were also measured.

Data for the TM polarization of the response of the MRR-OFT versus time and ethanol concentration are presented in Fig. 10; similar data hold for TE polarization. From the data of Fig. 10 for low concentrations, after partial ethanol pressure has been stabilized inside the chamber, a typical response time of this MRR-OFT vapor sensor is estimated to be less than 4min.

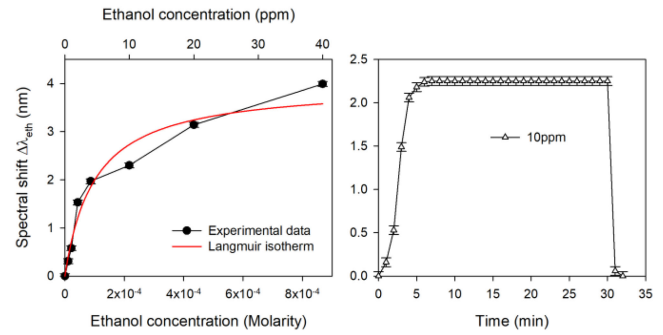


Fig. 11. (left) Ethanol vapor induced spectral shift $\Delta\lambda_{eth}$ versus ethanol concentration measured using the MRR-OFT system. (right) Ethanol vapor induced spectral shift $\Delta\lambda_{eth}$ response and recovery versus exposure time to ethanol of the MRR-OFT sensor. Experimental error for Molarity: 2.44×10^{-9} M.

Initially, for finding the role of ethanol vapor pressure into the transduction mechanism, the same MRR-OFT was subjected to inert gas pressure changes up to 14mbar, and insignificant spectral shifts of the WGM notches were recorded (less than 10pm); thus, gas pressure itself is not a principal transduction process. A deeper insight into the sensing transduction of the photo-polymerized MRR-OFTs can be obtained by the spectral shift $\Delta\lambda_{eth}$ introduced into the system versus concentration of the ethanol vapors, as this was extracted from saturated pressure and stabilized spectral shift values of Fig. 10; the trend of $\Delta\lambda_{eth}$ versus ethanol concentration is presented in Fig. 11. The TM polarisation data of Fig. 11 (left) were fitted using the Langmuir isotherm equation [31]:

$$\Delta\lambda_{eth} = \Delta\lambda_{max} \frac{K_L C_{eth}}{1 + K_L C_{eth}} \quad (1)$$

where $\Delta\lambda_{max}$ the maximum value of the wavelength shift measured, K_L the Langmuir equilibrium constant of adsorption with units of liters per mole and C_{eth} the molarity of ethanol vapors. The value of the K_L calculated from the fitted data, corresponds to a adsorption Gibbs energy change ΔG° of ~ 22.5 KJ/mol (where $\Delta G^\circ = -R \cdot T \cdot \ln[K_L \cdot \text{molarity units}]$, R the gas constant with a value of $8.314 \text{ J} \cdot \text{mol}^{-1} \cdot \text{K}^{-1}$ and T the temperature in Kelvin), showing a good agreement with data obtained for ethanol when adsorbed on porous silica surfaces of different hydrophobicity [32]. Deviations of the experimental data of Fig. 11 (left) observed for higher concentrations can be related to diffusion effects of the surface attached ethanol taking place into the photopolymerised resin; such a type of effects have been observed and exploited before [33]. In the present case, FEM simulations carried out while assuming a thin layer formed within a 20 nm depth into the MRR material with a $\sim 50\%$ volume porosity [33], reproduced a shift $\Delta\lambda_{eth} \sim 2.0$ nm of the WGM of Fig. 9 when this is fully adsorbed with ethanol. Finally, a significant characteristic of the MRR-OFT sensing device is related to its recovery behavior (see Fig. 11 right). By flushing the chamber with modest nitrogen overpressure (~ 1.1 bar), the spectral response of the device returns to its initial point within a typical time of ~ 2 min; exposure to ambient air again results in full recovery although with longer temporal response (~ 5 min).

Due to technical limitations, we could not perform ethanol vapor measurements using these MRR-OFT devices for concentrations lower than 0.5ppm. However, after considering the lower detection figure ($\Delta\lambda_{\text{eth}}^{0.5\text{ppm}} = 0.3 \text{ nm}$) obtained until now, ethanol vapor concentrations down to 100ppb are considered possible, by using the same resonators and wavelength resolution (0.05 nm) provided by the OSA.

IV. SUMMARY AND FUTURE WORK

We have presented the realization and characterization of a new type of micro-ring resonating devices attached onto optical fiber tapers, while their fabrication being enabled using MPL with a hybrid, organic-inorganic negative resin. The MRR-OFT devices presented exhibit Q-factors $\sim 2.5 \times 10^3$, sufficiently high for facilitating highly sensitive probing devices, while being exemplified into the detection of ethanol vapors down to concentrations of 0.5ppm, by exploiting reversible physisorption effects. Further investigations are focused on the fusion of both of the optical functionalities and elastic mechanical properties of these MRR-OFT, for the development of opto-mechanical oscillators.

ACKNOWLEDGMENT

VM, MF and SP would like to thank Aleka Manousaki for obtaining scanning electron microscopy pictures, as well as, Maria Konstantaki for assistance with optical fiber taper drawing.

REFERENCES

- [1] B. E. Little, S. T. Chu, H. A. Haus, J. Foresi, and J. P. Laine, "Microring resonator channel dropping filters," *J. Lightw. Technol.*, vol. 15, pp. 998–1005, 1997.
- [2] W. Bogaerts, *et al.*, "Silicon microring resonators," *Laser Photon. Rev.*, vol. 6, pp. 47–73, 2012.
- [3] Q. Xu, S. Sandhu, M. L. Povinelli, J. Shakya, S. Fan, and M. Lipson, "Experimental realization of an on-chip all-optical analogue to electromagnetically induced transparency," *Phys. Rev. Lett.*, vol. 96, pp. 123901, 2006.
- [4] D. A. Ketzaki, O. Tsilipakos, T. V. Yioultsis, and E. E. Kriezis, "Electromagnetically induced transparency with hybrid silicon-plasmonic traveling-wave resonators," *J. Appl. Phys.*, vol. 114, 2013, Art. no. 113107.
- [5] D. Urbonas *et al.*, "Ultra-wide free spectral range, enhanced sensitivity, and removed mode splitting SOI optical ring resonator with dispersive metal nanodisks," *Opt. Lett.*, vol. 40, pp. 2977–2980, Jul. 2015.
- [6] A. Canciamilla *et al.*, "Photo-induced trimming of coupled ring-resonator filters and delay lines in As₂S₃ chalcogenide glass," *Opt. Lett.*, vol. 36, pp. 4002–4004, 2011.
- [7] M. A. Bandres *et al.*, "Topological insulator laser: Experiments," *Science*, vol. 359, 2018, Art. no. eaar4005.
- [8] M. Iqbal, *et al.*, "Label-Free biosensor arrays based on silicon ring resonators and high-speed optical scanning instrumentation," *IEEE J. Sel. Topics Quantum Electron.*, vol. 16, no. 3, pp. 654–661, May 2010.
- [9] X. Jiang, *et al.*, "Demonstration of microfiber knot laser," *Appl. Phys. Lett.*, vol. 89, Oct. 2006, Art. no. 143513.
- [10] K. Kosma, G. Zito, K. Schuster, and S. Pissadakis, "Whispering gallery mode microsphere resonator integrated inside a microstructured optical fiber," *Opt. Lett.*, vol. 38, pp. 1301–1303, 2013.
- [11] K. Kosma, K. Schuster, J. Kobelke, and S. Pissadakis, "An 'in-fiber' whispering-gallery-mode bi-sphere resonator, sensitive to nanometric displacements," *Appl. Phys. B*, vol. 124, 2018.
- [12] X. Jiang, Y. Chen, G. Vienne, and L. Tong, "All-fiber add-drop filters based on microfiber knot resonators," *Opt. Lett.*, vol. 32, pp. 1710–1712, Jun. 15, 2007.
- [13] J.-L. Kou, J. Feng, L. Ye, F. Xu, and Y.-Q. Lu, "Miniaturized fiber taper reflective interferometer for high temperature measurement," *Opt. Exp.*, vol. 18, pp. 14245–14250, 2010.
- [14] Y. Ran, *et al.*, "193 nm excimer laser inscribed Bragg gratings in microfibers for refractive index sensing," *Opt. Exp.*, vol. 19, pp. 18577–18583, 2011.
- [15] A. Camposeo, L. Persano, M. Farsari, and D. Pisignano, "Additive manufacturing: Applications and directions in photonics and optoelectronics," *Adv. Opt. Mater.*, vol. 7, 2019, Art. no. 1800419.
- [16] M. Malinauskas, *et al.*, "Laser fabrication of various polymer microoptical components," *Eur. Phys. J. Appl. Phys.*, vol. 58, 2012, Art. no. 20501.
- [17] A. Bertoncini and C. Liberale, "3D printed waveguides based on photonic crystal fiber designs for complex fiber-end photonic devices," *Optica*, vol. 7, pp. 1487–1494, Nov. 2020.
- [18] M. Malinauskas, A. Žukauskas, G. Bičkauskaitė, R. Gadonas, and S. Juodkaziš, "Mechanisms of three-dimensional structuring of photopolymers by tightly focussed femtosecond laser pulses," *Opt. Exp.*, vol. 18, pp. 10209–10221, May 10, 2010.
- [19] O. Tsilipakos, *et al.*, "Split-cube-resonator-based metamaterials for polarization-selective asymmetric perfect absorption," *Sci. Rep.*, vol. 10, Oct. 2020, Art. no. 17653.
- [20] T. Gissibl, M. Schmid, and H. Giessen, "Spatial beam intensity shaping using phase masks on single-mode optical fibers fabricated by femtosecond direct laser writing," *Optica*, vol. 3, pp. 448–451, Apr. 2016.
- [21] V. Melissinaki, M. Farsari, and S. Pissadakis, "A fiber-endface, fabry-perot vapor microsensor fabricated by multiphoton polymerization," *IEEE J. Sel. Topics Quantum Electron.*, vol. 21, no. 4, pp. 344–353, Jul. 2015.
- [22] Z. Li, C. Liao, J. Wang, P. Zhou, and Y. Wang, "Femtosecond laser micro-printing of a fiber whispering gallery mode resonator for highly-sensitive temperature measurements," *J. Lightw. Technol.*, vol. 37, pp. 1241–1245, 2019.
- [23] V. Melissinaki, M. Farsari, and S. Pissadakis, "A fiber optic fabry-perot cavity sensor for the probing of oily samples," *Fibers*, vol. 5, pp. 1, 2017.
- [24] O. Tsilipakos, T. V. Yioultsis, and E. E. Kriezis, "Theoretical analysis of thermally tunable microring resonator filters made of dielectric-loaded plasmonic waveguides," *J. Appl. Phys.*, vol. 106, Nov. 2009, Art. no. 093109.
- [25] M. Cai, O. Painter, and K. J. Vahala, "Observation of critical coupling in a fiber taper to a silica-microsphere whispering-gallery mode system," *Phys. Rev. Lett.*, vol. 85, pp. 74–77, 2000.
- [26] C. Elosua, R. I. Matias, C. Barriain, and J. F. Arregui, "Volatile organic compound optical fiber sensors: A review," *Sensors*, vol. 6, 2006.
- [27] N. A. Yebo, P. Lommens, Z. Hens, and R. Baets, "An integrated optic ethanol vapor sensor based on a silicon-on-insulator microring resonator coated with a porous ZnO film," *Opt. Exp.*, vol. 18, pp. 11859–11866, 2010.
- [28] M. Konstantaki, A. Klini, D. Anglos, and S. Pissadakis, "An ethanol vapor detection probe based on a ZnO nanorod coated optical fiber long period grating," *Opt. Exp.*, vol. 20, pp. 8472–8484, 2012.
- [29] S. Nair, K. Cope, R. H. Terence, and A. M. Diehl, "Obesity and female gender increase breath ethanol concentration: Potential implications for the pathogenesis of nonalcoholic steatohepatitis," *Am. J. Gastroenterol.*, vol. 96, pp. 1200–1204, 2001.
- [30] A. G. Dent, T. G. Sutedja, and P. V. Zimmerman, "Exhaled breath analysis for lung cancer," *J. Thoracic Dis.*, pp. S540–S550, 2013.
- [31] Y. Liu, "Is the free energy change of adsorption correctly calculated?," *J. Chem. Eng. Data*, vol. 54, pp. 1981–1985, 2009.
- [32] D. Wu, X. Guo, H. Sun, and A. Navrotsky, "Energy landscape of water and ethanol on silica surfaces," *J. Phys. Chem. C*, vol. 119, pp. 15428–15433, Jul. 2015.
- [33] V. Melissinaki, I. Konidakis, M. Farsari, and S. Pissadakis, "Fiber endface fabry-perot microsensor with distinct response to vapors of different chlorinated organic solvents," *IEEE Sensors J.*, vol. 16, pp. 7094–7100, 2016.

Vasileia Melissinaki was born in Heraklion, Crete, Greece, in 1985. She received the B.S. degree in physics from the Department of Physics, University of Crete, Greece, in 2009, the M.S. degree in microelectronics and optoelectronics in 2011, and the Ph.D. degree in 2017 from the same department. She is currently a Postdoctoral Fellow with the Institute of Electronic Structure and Laser (IESL) in Foundation for Research and Technology-Hellas (FORTH). From 2009 to 2013, she was a Teaching Assistant in undergraduate Physics Laboratories with the Department of Physics, University of Crete. She is a coauthor of 11 journal and 16 conference publications, two book chapters. Her research interest includes the fabrication and study of 3D micro-optical elements, the development of 3D scaffolds for tissue engineering and micro-implants for medical applications using laser photo-polymerization techniques, and the development of optical fiber devices using advanced laser techniques.

Odysseas Tsilipakos (Senior Member, IEEE) received the Diploma and Ph.D. degrees from the Department of Electrical and Computer Engineering, Aristotle University of Thessaloniki (AUTH) in 2008 and 2013, respectively. From 2014 to 2015, he was a Postdoctoral Research Fellow with AUTH. Since 2016, he is a Postdoctoral Researcher with the Institute of Electronic Structure and Laser (IESL) in Foundation for Research and Technology Hellas (FORTH). His research interests span metasurfaces and metamaterials, plasmonics and nanophotonics, resonators and cavities, nonlinear optics in resonant structures and waveguides, 2D photonic materials, and theoretical and computational electromagnetics. He has authored or coauthored of 37 publications in refereed journals and of 50 publications in international conferences. He was the recipient of Best Student Paper Award in SPIE Photonics Europe 2012. He is a member of The Optical Society (OSA).

Maria Kafesaki received the Ph.D. degree in 1997 from the Physics Department of the University of Crete, Greece, on elastic wave propagation in complex media. She is an Associate Professor with the Department of Materials Science and Technology of the University of Crete and an Adjunct Researcher with the Institute of Electronic Structure and Laser (IESL) of the Foundation for Research and Technology Hellas (FORTH). She has worked as a Postdoctoral Researcher with the Consejo Superior de Investigaciones Cientificas in Madrid, Spain, and in IESL of FORTH (1997–2001). Her current research is on the area of electromagnetic wave propagation in periodic and random media, with emphasis on photonic crystals and metamaterials, where she has large theoretical and computational experience. She has more than 110 publications in refereed journals (with more than 6500 citations and h-index = 42, according to Web of Science), and more than 70 invited talks at international conferences and schools. She has participated in many European projects as well as in the organization of many international conferences and schools. She is Fellow of the Optical Society of America.

Maria Farsari is a Research Director with FORTH/IESL and the Leader of the NLL group. She has authored or coauthored more than 100 papers in refereed journals, she has received more than 5900 citations. Her h-index is 44. Her research activities focus on laser-matter interactions and ultra-fast laser materials processing. She is particularly active in the field of multiphoton polymerization, where she is one of the world leaders in the fabrication and characterization of 3D micro- and nanostructures for applications in photonics, metamaterials and biomedicine. Dr. Farsari has participated in many FP6, FP7 & H2020 European research projects, and national projects also. Her group consists of three Postdoctoral Research Scientist, three Ph.D. students, one M.Sc. student, and one undergraduate.

Stavros Pissadakis received the Ptychion degree from the Physics Department of the University of Crete, Greece, in 1994 and the Ph.D. degree from Optoelectronics Research Centre (ORC), University of Southampton, U.K., in 2000. He is Director of Research with the Foundation for Research and Technology-Hellas (FORTH), Institute of Electronic Structure and Laser (IESL). He has been employed in several academic positions in Greece and U.K. recently, he was a Visiting Professor with the University of Parma, Italy. On year 2003, he joined FORTH-IESL, where he established the Photonic Materials and Devices Laboratory (PMDL). He has coordinated/participated in several European and National research and industrial projects, also, he is a member of the Board of Stakeholders of the European Technological Platform Photonics21. His current scientific interests include development of microstructured and photonic crystal fiber switching and sensing devices, optofluidics, whispering gallery mode devices, and study of photosensitivity in optical fibers and materials using laser radiation. Dr. Pissadakis has authored or coauthored 74 publications in refereed journals and of 135 publications in international conferences, including 40 invited contributions. He is a Topical Editor of Applied Optics, a Member of IEEE and a Senior Member of OSA.